J. Mod. Power Syst. Clean Energy (2019) 7(2):350–356
https://doi.org/10.1007/s40565-018-0402-8

Fault diagnosis of wind turbine bearing based on stochastic subspace identification and multi-kernel support vector machine

Hongshan ZHAO[1], Yufeng GAO[1], Huihai LIU[1], Lang LI[1]

Abstract In order to accurately identify a bearing fault on a wind turbine, a novel fault diagnosis method based on stochastic subspace identification (SSI) and multi-kernel support vector machine (MSVM) is proposed. First, the collected vibration signal of the wind turbine bearing is processed by the SSI method to extract fault feature vectors. Then, the MSVM is constructed based on Gauss kernel support vector machine (SVM) and polynomial kernel SVM. Finally, fault feature vectors which indicate the condition of the wind turbine bearing are inputted to the MSVM for fault pattern recognition. The results indicate that the SSI-MSVM method is effective in fault diagnosis for a wind turbine bearing and can successfully identify fault types of bearing and achieve higher diagnostic accuracy than that of *K*-means clustering, fuzzy means clustering and traditional SVM.

Keywords Wind turbine, Bearing, Fault diagnosis, Stochastic subspace identification (SSI), Multi-kernel support vector machine (MSVM)

CrossCheck date: 27 February 2018

Received: 22 October 2017 / Accepted: 27 February 2018 / Published online: 4 April 2018

✉ Huihai LIU
hhliu3@126.com

Hongshan ZHAO
zhaohshcn@126.com

Yufeng GAO
gaoyf945@163.com

Lang LI
li1lang@163.com

[1] School of Electrical and Electronic Engineering, North China Electric Power University, Baoding, China

1 Introduction

Recent decades renewable energy sources have received increasingly wide attention. As one of the most promising new clean renewable energy sources, wind power generation is in large-scale development around the world [1–4]. However, wind turbines are prone to various failures due to long-term operation under tough conditions, complex alternating loads and variable speeds [5]. The bearing is a critical component of a wind turbine and bearing failures form a significant proportion of all failures in wind turbines. These, can lead to outage of the unit and a high maintenance cost [6, 7]. Hence, the development of an accurate fault diagnosis method for wind turbine bearing would be extremely valuable for improving safety and economy.

Vibration analysis is an effective condition monitoring method, especially suitable for rotating machinery. So far, a vast number of vibration signal processing methods have been used in fault detection of the gear box and bearing for wind turbines, such as spectrum analysis [8], wavelet transform [9], Wigner-Vile distribution [10] and empirical mode decomposition (EMD) [11]. Compared with the former three methods, EMD performs better in processing the vibration signal but it has the drawback of being time-consuming [12]. Variational mode decomposition (VMD) [13] and empirical wavelet transform (EWT) [14] achieve better signal processing performance than EMD and avoid mode aliasing, and they have strong noise robustness. In the past 20 years, the application of the stochastic subspace identification (SSI) method in vibration signal analysis has also developed very fast [15, 16], especially in the fault diagnosis field related to buildings and rotating equipment [17, 18]. However, the SSI method has so far seldom been used to diagnose a bearing fault for a wind turbine. The SSI method directly constructs a model based on time-domain data and can identify the mode parameters. This is suitable for mining the most essential fault information [19]. In this paper, SSI is employed to extract fault features by processing the collected vibration signal of the wind turbine.

In recent years, intelligent diagnosis methods have been widely applied in diagnosing a bearing fault in a wind turbine. As one of the artificial intelligence methods, the support vector machine (SVM) has many special advantages in solving with small samples, nonlinear and high dimensional pattern recognition. Reference [20] used SVM to classify different states of a rolling bearing and conducted experiments to validate the effectiveness of the proposed method. Reference [21] proposed a method based on wavelet packet and a locally linear embedding algorithm to extract fault features, and then intelligently classified the different fault degrees of a rolling bearing using SVM. Reference [22] combined EMD and SVM to identify different fault states of a rolling bearing. A single kernel function is used in the traditional SVM method to solve the classification problem of simple data. However, traditional SVM cannot effectively solve a complex classification problem, especially for a heterogeneous and imbalanced data classification problem. In order to improve the performance of SVM, a multi-kernel support vector machine (MSVM) is adopted for pattern recognition in this paper. MSVM not only integrates the generalization ability but also the self-learning ability of the traditional single kernel SVM [23–25], thus having better adaptability and robustness.

We use wind turbine bearing vibration data to construct the subspace model and to realize the bearing feature extraction, then use the MSVM algorithm to classify the feature parameters for bearing fault diagnosis. The paper is organized as follows. The principles of SSI and MSVM are respectively introduced in Section 2 and Section 3. The procedure of fault diagnosis method based on SSI-MSVM is described in Section 4. Diagnostic performance is tested by applying the SSI-MSVM method to a bearing experimental signal of a wind turbine in Section 5. Finally, conclusions are drawn in Section 6.

2 Principle of SSI

2.1 Stochastic state-space model

The SSI method is a black box identification method using collected data to establish a linear state space model, and is very suitable for extracting features of vibration signals. The stochastic state-space model can be described as follows:

$$\begin{cases} \boldsymbol{X}_{k+1} = \boldsymbol{A}\boldsymbol{X}_k + \boldsymbol{w}_k \\ \boldsymbol{Y}_k = \boldsymbol{C}\boldsymbol{X}_k + \boldsymbol{v}_k \end{cases} \tag{1}$$

where $\boldsymbol{X}_k \in \mathbf{R}^n$ and $\boldsymbol{Y}_k \in \mathbf{R}^l$ are the state variable and output of the system in discrete time k, respectively; $\boldsymbol{A} \in \mathbf{R}^{n \times n}$ is the system matrix, which describes the dynamic behaviour of the system; $\boldsymbol{C} \in \mathbf{R}^{l \times n}$ is the output matrix of the system; $\boldsymbol{w}_k \in \mathbf{R}^n$ and $\boldsymbol{v}_k \in \mathbf{R}^l$ are system noise and measurement noise, respectively.

2.2 SSI method

The SSI method can be completed in three steps: orthogonal projection, singular value decomposition and system parameter estimation.

2.2.1 *Orthogonal projection*

First, a block Hankel matrix $\boldsymbol{Y}$ composed of the measurement signal is defined as follows:

$$\boldsymbol{Y} \triangleq \left[\begin{array}{cccc} y_1 & y_2 & \cdots & y_N \\ y_2 & y_3 & \cdots & y_{N+1} \\ \vdots & \vdots & & \vdots \\ y_i & y_{i+1} & \cdots & y_{i+N-1} \\ \hdashline y_{i+1} & y_{i+2} & \cdots & y_{i+N} \\ y_{i+2} & y_{i+3} & \cdots & y_{i+N+1} \\ \vdots & \vdots & & \vdots \\ y_{i+j+1} & y_{i+j+2} & \cdots & y_{i+j+N} \end{array}\right] = \left[\begin{array}{c} \boldsymbol{Y}_{1|i} \\ \hdashline \boldsymbol{Y}_{i+1|i+j+1} \end{array}\right] = \left[\begin{array}{c} \boldsymbol{Y}_p \\ \hdashline \boldsymbol{Y}_f \end{array}\right] \tag{2}$$

where y_k (k=1, 2, …, i+j+N) is the collected signal; $\boldsymbol{Y}_p$ is the past part in matrix $\boldsymbol{Y}$ and its row number is i; $\boldsymbol{Y}_f$ is the future part in matrix $\boldsymbol{Y}$ and its row number is j+1; both i and j are generally not less than the maximum order of the system model, namely, $\min\{i, j+1\} \geq n$; and the column number of the block Hankel matrix $\boldsymbol{N}$ is generally far greater than i and j+1, namely, $N \gg \max\{i, j+1\}$.

Matrix $\boldsymbol{Y}$ is newly divided into two blocks as follows:

$$\boldsymbol{Y} \triangleq \left[\begin{array}{cccc} y_1 & y_2 & \cdots & y_N \\ y_2 & y_3 & \cdots & y_{N+1} \\ \vdots & \vdots & & \vdots \\ y_i & y_{i+1} & \cdots & y_{i+N-1} \\ y_{i+1} & y_{i+2} & \cdots & y_{i+N} \\ \hdashline y_{i+2} & y_{i+3} & \cdots & y_{i+N+1} \\ \vdots & \vdots & & \vdots \\ y_{i+j+1} & y_{i+j+2} & \cdots & y_{i+j+N} \end{array}\right] = \left[\begin{array}{c} \boldsymbol{Y}_{1|i+1} \\ \hdashline \boldsymbol{Y}_{i+2|i+j+1} \end{array}\right] = \left[\begin{array}{c} \boldsymbol{Y}_p^+ \\ \hdashline \boldsymbol{Y}_f^- \end{array}\right] \tag{3}$$

where $\boldsymbol{Y}_p^+$ is the new past part generated by shifting the first row of $\boldsymbol{Y}_f$ into the last row of $\boldsymbol{Y}_p$; $\boldsymbol{Y}_f^-$ is the new future part generated by deleting the last row of $\boldsymbol{Y}_f$.

$\boldsymbol{Y}_f$ is orthogonally projected to the space of $\boldsymbol{Y}_p$ by the following equation:

$$\boldsymbol{P}_m \triangleq \frac{\boldsymbol{Y}_f}{\boldsymbol{Y}_p} = \boldsymbol{Y}_f\boldsymbol{Y}_p^{\mathrm{T}}\left(\boldsymbol{Y}_p\boldsymbol{Y}_p^{\mathrm{T}}\right)^{\dagger}\boldsymbol{Y}_p \tag{4}$$

where $(\bullet)^{\dagger}$ denotes the Moore-Penrose inverse matrix.

Similarly, $\boldsymbol{Y}_f^-$ is orthogonally projected to the space of $\boldsymbol{Y}_p^+$ as follows:

$$\boldsymbol{P}_{m-1} \triangleq \frac{\boldsymbol{Y}_f^-}{\boldsymbol{Y}_p^+} = \boldsymbol{Y}_f^-\left(\boldsymbol{Y}_p^+\right)^{\mathrm{T}}\left(\boldsymbol{Y}_p^+\left(\boldsymbol{Y}_p^+\right)^{\mathrm{T}}\right)^{\dagger}\boldsymbol{Y}_p^+ \tag{5}$$

2.2.2 Singular value decomposition

Singular value decomposition is adopted to analyze the projection matrix $\boldsymbol{P}_m$ as follows:

$$\boldsymbol{P}_m = [\boldsymbol{U}_1 \quad \boldsymbol{U}_0]\begin{bmatrix}\boldsymbol{S}_1 & \boldsymbol{0}\\ \boldsymbol{0} & \boldsymbol{S}_0\end{bmatrix}\begin{bmatrix}\boldsymbol{V}_1^{\mathrm{T}}\\ \boldsymbol{V}_0^{\mathrm{T}}\end{bmatrix} \tag{6}$$

where $\boldsymbol{U}_1$ and $\boldsymbol{V}_1$ are unitary matrices; $\boldsymbol{S}_1 = \mathrm{diag}\{\sigma_1, \sigma_2, \cdots, \sigma_i, \cdots, \sigma_n\}$ is the diagonal matrix and σ_i is the ith singular value of $\boldsymbol{S}_1$; $\boldsymbol{U}_0$, $\boldsymbol{V}_0$, $\boldsymbol{S}_0$ are null matrices.

The projection matrix $\boldsymbol{P}_m$ can also be expressed as the product of the observable matrix $\boldsymbol{\Gamma}_m$ and the Kalman filter sequence $\hat{\boldsymbol{X}}_m$.

$$\boldsymbol{P}_m = \boldsymbol{\Gamma}_m\hat{\boldsymbol{X}}_m \tag{7}$$

Similarly, the rejection matrix $\boldsymbol{P}_{m-1}$ can also be expressed as follows:

$$\boldsymbol{P}_{m-1} = \underline{\boldsymbol{\Gamma}}_m\hat{\boldsymbol{X}}_{m+1} \tag{8}$$

Where $\underline{\boldsymbol{\Gamma}}_m$ is the new observable matrix generated by deleting the last row of $\boldsymbol{\Gamma}_m$.

According to (6) and (7), the observable matrix $\boldsymbol{\Gamma}_m$ and the state variable $\hat{\boldsymbol{X}}_m$ can be inferred.

$$\boldsymbol{\Gamma}_m = \boldsymbol{U}_1\boldsymbol{S}_1^{\frac{1}{2}} \tag{9}$$

$$\hat{\boldsymbol{X}}_m = \boldsymbol{S}_1^{\frac{1}{2}}\boldsymbol{V}_1^{\mathrm{T}} \tag{10}$$

The state variable $\hat{\boldsymbol{X}}_{m+1}$ can also be obtained from (8),

$$\hat{\boldsymbol{X}}_{m+1} = (\underline{\boldsymbol{\Gamma}}_m)^{\dagger}\boldsymbol{P}_{m-1} \tag{11}$$

2.2.3 System parameter estimation

By plugging state variable $\hat{\boldsymbol{X}}_m$ and $\hat{\boldsymbol{X}}_{m+1}$ into the stochastic state-space model, the following formula can be obtained:

$$\begin{bmatrix}\hat{\boldsymbol{X}}_{m+1}\\ \boldsymbol{Y}_{m|m}\end{bmatrix} = \begin{bmatrix}\boldsymbol{A}\\ \boldsymbol{C}\end{bmatrix}\hat{\boldsymbol{X}}_m + \begin{bmatrix}\boldsymbol{\rho}_w\\ \boldsymbol{\rho}_v\end{bmatrix} \tag{12}$$

where $\boldsymbol{\rho}_w$ and $\boldsymbol{\rho}_v$ are residual vectors and not related to $\hat{\boldsymbol{X}}_m$.

Then the system matrix $\boldsymbol{A}$ and output matrix $\boldsymbol{C}$ can be estimated by applying the least squares method as follows:

$$\begin{bmatrix}\boldsymbol{A}\\ \boldsymbol{C}\end{bmatrix} \approx \begin{bmatrix}\hat{\boldsymbol{A}}\\ \hat{\boldsymbol{C}}\end{bmatrix} = \begin{bmatrix}\hat{\boldsymbol{X}}_{m+1}\\ \boldsymbol{Y}_{m|m}\end{bmatrix}(\hat{\boldsymbol{X}}_m)^{\dagger} \tag{13}$$

where $\hat{\boldsymbol{A}}$ and $\hat{\boldsymbol{C}}$ denote the estimates of $\boldsymbol{A}$ and $\boldsymbol{C}$, respectively.

In (13), the matrix $\boldsymbol{A}$ contains the feature information of the system model built by the bearing vibration data. That is, the eigenvalues of matrix $\boldsymbol{A}$ correspond to different fault modes.

The eigenvalue decomposition of the matrix $\boldsymbol{A}$ is given by:

$$\boldsymbol{A} = \boldsymbol{U}\boldsymbol{\Sigma}\boldsymbol{V}^{\mathrm{T}} \tag{14}$$

where $\boldsymbol{U}$ is the left singular matrix of the system matrix $\boldsymbol{A}$; $\boldsymbol{V}^{\mathrm{T}}$ is the transpose of the right singular matrix of the system matrix $\boldsymbol{A}$; $\boldsymbol{\Sigma} = \mathrm{diag}\{\lambda_1, \lambda_2, \cdots, \lambda_n\}$ is a diagonal matrix and λ_i is the ith singular value of the system matrix $\boldsymbol{A}$.

3 Principles of standard SVM and MSVM

3.1 Standard SVM

The basic principle of the SVM is to map the input samples from original space to high dimensional feature space by a kernel function. Given a sample set$\{(\boldsymbol{x}_1, y_1), (\boldsymbol{x}_2, y_2), \cdots, (\boldsymbol{x}_n, y_n)\}$, where $\boldsymbol{x}_i \in \mathbf{R}^n$ is the input samples and $y_i \in \{-1, +1\}$ is the output samples, SVM maps the input samples to the n dimensional feature space using the kernel function, in which the optimal classification hyper plane $\sum_{i=1}^{n} w_i k(\boldsymbol{x}, \boldsymbol{x}_i)$ is constructed, where w_i is the ith element of the coefficient vector $\boldsymbol{w}$. The classification interval in optimal hyper plane 2/||$\boldsymbol{w}$|| is expected to achieve a maximum in the SVM method. By introducing slack variables, the optimal hyper plane is transformed into the following constrained optimization problem:

$$\begin{cases}\min\ J(\boldsymbol{w}, \boldsymbol{e}) = \dfrac{1}{2}\boldsymbol{w}^{\mathrm{T}}\boldsymbol{w} + C\displaystyle\sum_{i=1}^{n} e_i^2\\ \text{s.t.}\ \ y_i(\boldsymbol{w}^{\mathrm{T}}\boldsymbol{\phi}(\boldsymbol{x}_i) + b) \geq 1 - e_i\\ \qquad e_i \geq 0\end{cases} \tag{14}$$

where $i = 1, 2, \cdots, n$; e_i is the ith element of the slack variable vector $\boldsymbol{e}$; C is penalty coefficient; b denotes the distance from the hyper plane to the origin; $\boldsymbol{\phi}(\cdot)$ is mapping function.

The Lagrange multiplier α_i is used to transform the constrained optimization problem into the dual optimization problem. Thus, the final classification decision function is described as follows:

$$f(\boldsymbol{x}) = \operatorname{sgn}\left(\sum_{i=1}^{n} y_i \alpha_i k(\boldsymbol{x}, \boldsymbol{x}_i) + b\right) \tag{15}$$

3.2 MSVM

In the process of fault identification using the SVM, the selection of kernel function is a key segment. Different kernel functions correspond to different discriminant functions, which directly affect the identification accuracy of the SVM. The kernel functions of the SVM mainly include a local kernel function and a global kernel function. And the Gauss kernel function is a typical local kernel function and can be described as follows:

$$K_{RBF}(\boldsymbol{x}_i, \boldsymbol{x}_j) = \exp\left(\frac{-\left\|\boldsymbol{x}_i - \boldsymbol{x}_j\right\|}{\sigma^2}\right) \tag{16}$$

where σ is the kernel parameter.

As a typical global kernel function, the polynomial kernel function can be described as follows:

$$K_{ploy}(\boldsymbol{x}_i, \boldsymbol{x}_j) = \left(\boldsymbol{x}_i^{\mathrm{T}} \boldsymbol{x}_j + 1\right)^d \tag{17}$$

where d is the kernel parameter.

A single kernel function is used in the traditional SVM method and can solve the classification problem of simple data. However, the traditional SVM has some limitations for a complex classification problem such as bearing fault diagnosis. In order to improve the performance of the SVM, it is proposed to combine the local and global kernels to construct the MSVM, which can be described as follows:

$$K_{\min}(\boldsymbol{x}_i, \boldsymbol{x}_j) = \lambda K_{RBF}(\boldsymbol{x}_i, \boldsymbol{x}_j) + (1-\lambda) K_{ploy}(\boldsymbol{x}_i, \boldsymbol{x}_j) \tag{18}$$

where λ ($0<\lambda<1$) is the tuning parameter.

According to (18), it can be readily seen that the multi-kernel function degenerates into the Gauss kernel function under the condition that λ=0 and into the polynomial kernel function under the condition that λ=1. The multi-kernel function can adapt to different input samples by adjusting the tune parameter λ. The MSVM integrates prior knowledge of specific problems in the process of selecting the kernel function, and thus it has the ability of learning and generalization combined.

4 Fault diagnosis model based on SSI method and MSVM

In this section, a novel fault diagnosis method based on SSI-MSVM is proposed for the wind turbine bearing. The flow chart of the SSI-MSVM method is shown in Fig. 1.

The detailed procedure is described as follows:

1) Vibration signal acquisition. Setting the mounting position of vibration sensors and sampling rate, the vibration signal of the wind turbine bearing is acquired through a signal acquisition system.
2) SSI analysis. First, the collected vibration signal is used to construct a stochastic state-space model of a wind turbine bearing as shown in (1). Then, the SSI method is applied to estimate the system matrix $\boldsymbol{A}$, eigenvalues of which are extracted as fault feature vectors.
3) Training MSVM model. Samples in different states are taken as training samples to train the MSVM, establishing the fault diagnosis model. The trained model can be used to distinguish different patterns.
4) Fault diagnosis. The test samples are input to the trained fault diagnosis model for classification, and the working state and fault type of the wind turbine bearing can be determined according to the output of the MSVM model.

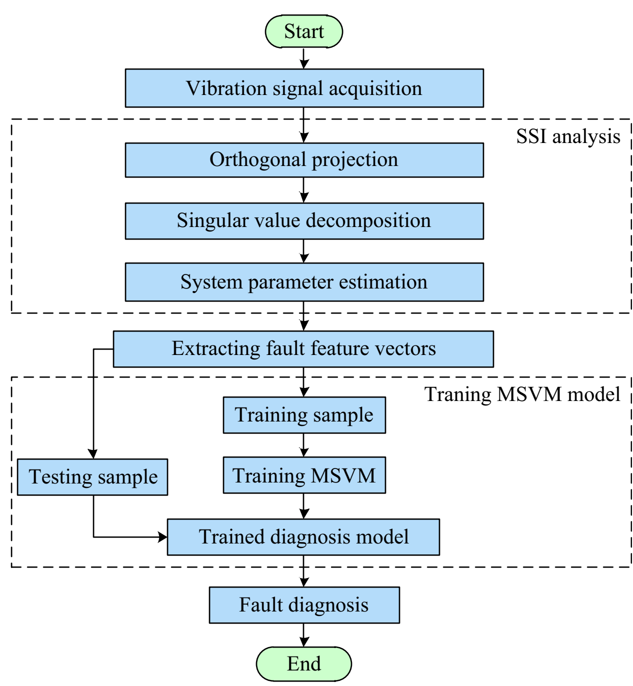

Fig. 1 Flow chart of fault diagnosis method for bearing based on SSI-MSVM

5 Experiment analysis

To validate the practicability and effectiveness of SSI-MSVM in fault diagnosis, bearing fault experiments are conducted in a wind turbine test rig, which is shown in Fig. 2. The test rig is composed of wheel hub, main shaft, gearbox and generator. The main shaft is supported by two rolling bearings, which bear mainly the radial and also a certain axial load. An acceleration sensor, X&K AD500T, is mounted on the bearing pedestal to acquire vibration signals and the sampling frequency is 10 kHz. Parameters of X&K AD500T are as follows: measuring range of $25g$ ($g = 9.8$ m/s^2), sensitivity of 500 mV per g, frequency range of 0.3-12000 Hz and resolution of $0.004g$. To simulate the typical faults of a wind turbine bearing, a spark erosion technique is used to seed a pit in the inner race, roller and outer race.

In Figs. 3 and 4, the two sets of vibration signals are collected from wind turbine bearings in different conditions. They respectively simulate strong fault and weak fault modes of the bearing. Compared with the time waveform of the normal vibration signal, it can be seen that there are irregular and large amplitude shock signals in strong faults in Fig. 3, but in Fig. 4 the shock signals of weak faults are not obvious.

For the SSI method, the length of each data sample should be long enough to satisfy the validity of fault feature extraction. So, each sample is set to contain 9000 data points in processing the vibration signal of the wind turbine bearing. Both the Hankel matrix $\boldsymbol{Y}_p$ and $\boldsymbol{Y}_f$ are 9×8991 dimensional matrices. The projection matrix is analysed by singular value decomposition and the results indicate that

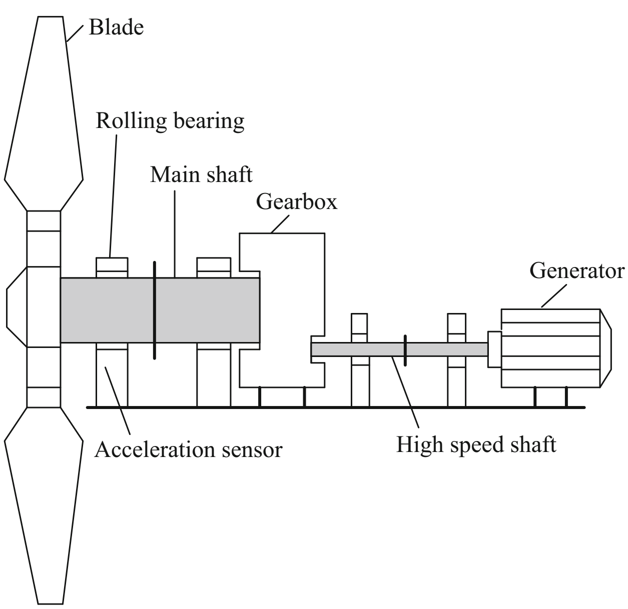

Fig. 2 Structure diagram of wind turbine test rig

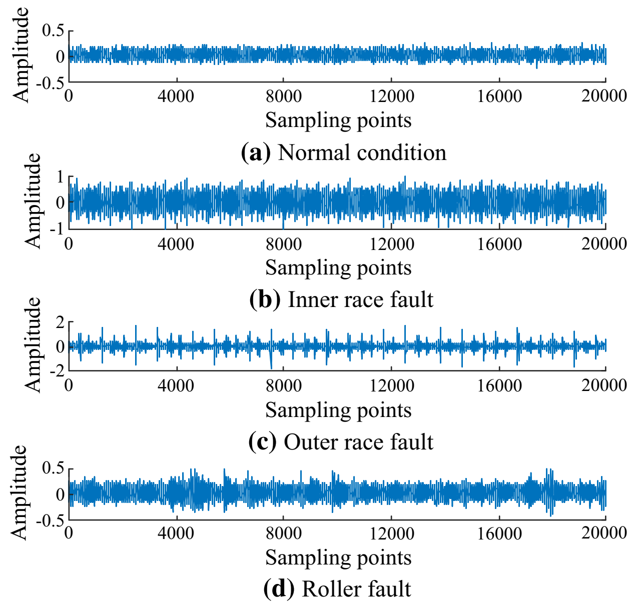

Fig. 3 Time waveform of bearing vibration signal in normal and strong faults

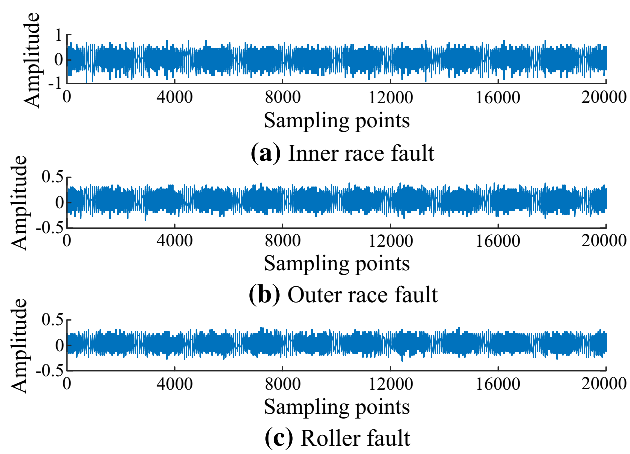

Fig. 4 Time waveform of bearing vibration signal in weak faults

the order of the stochastic subspace model is 5. Then the SSI method is applied to process the collected signal and eigenvalues of the system matrix are obtained. Figure 5 shows the features of the bearing vibration signal in different conditions extracted by the SSI model. It can be seen that all the eigenvalues are distributed in the unit circle, which indicates that the identified bearing stochastic subspace model is stable and effective. At the same time, the distributed locations of eigenvalue corresponding to normal mode and different fault modes are non-coincident which illustrates that these different eigenvalues can be discriminated by a clustering algorithm.

For strong faults and weak faults of bearing in this study, 320 samples gained from an experimental roller

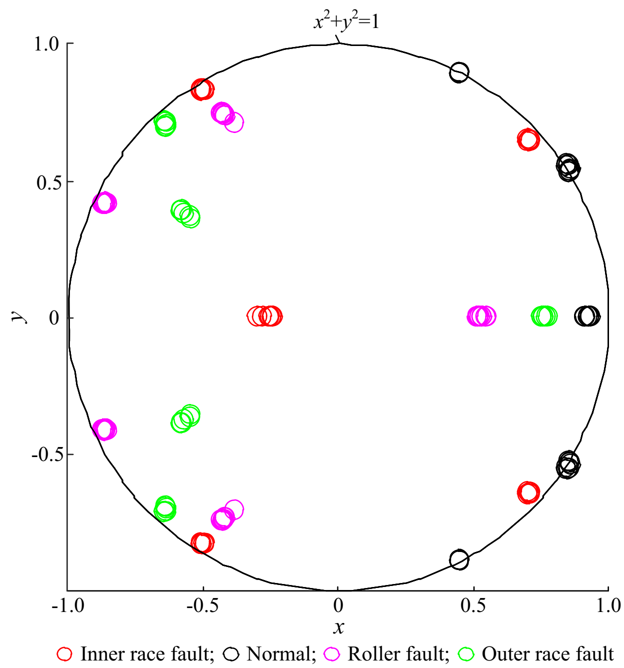

Fig. 5 Features extracted by SSI in different conditions

bearing are respectively adopted to verify the superior diagnostic performance of the SSI-MSVM method compared with that of *K*-means clustering, fuzzy means clustering (FCM) and traditional SVM. All data are divided into two data sets: the training and test, in which the training data sets including 120 samples are used to calculate the fitness function and train the diagnosis model, and the test data sets are used to examine the classification accuracy of each model.

In order to prove the stability of the experiment, six groups of comparative experiments with different unlabeled testing sample sets are operated. Each experiment is carried out 10 times. The average test accuracies of different pattern identification methods are presented in Table 1. Figure 6 shows the visual expression of the comparison result between the proposed method and other methods.

From Table 1 and Fig. 6, it can be seen that the fault diagnosis accuracy of the SSI-MSVM method is in the range of 90.27%-92.73%, while that of *K*-means clustering, FCM and SVM are in the range of 82.53%-88.06%, 86.35%-89.32% and 89.25%-91.03%, respectively. Overall, the SSI-MSVM method has a higher diagnostic accuracy than that of *K*-means clustering, FCM and SVM, which indicates that the proposed diagnosis model is clearly superior to the traditional diagnosis method.

Table 1 Fault diagnosis result comparison among *K*-means clustering, FCM, SVM and MSVM

No.	Total samples	Classification accuracy (%)			
		K-means	FCM	SVM	MSVM
1	40	82.53	86.35	89.25	90.27
2	80	86.27	88.05	91.03	91.46
3	120	87.73	89.02	90.75	92.72
4	160	88.06	89.03	90.81	92.73
5	200	87.71	89.02	90.76	92.47
6	240	87.75	89.32	89.82	92.35

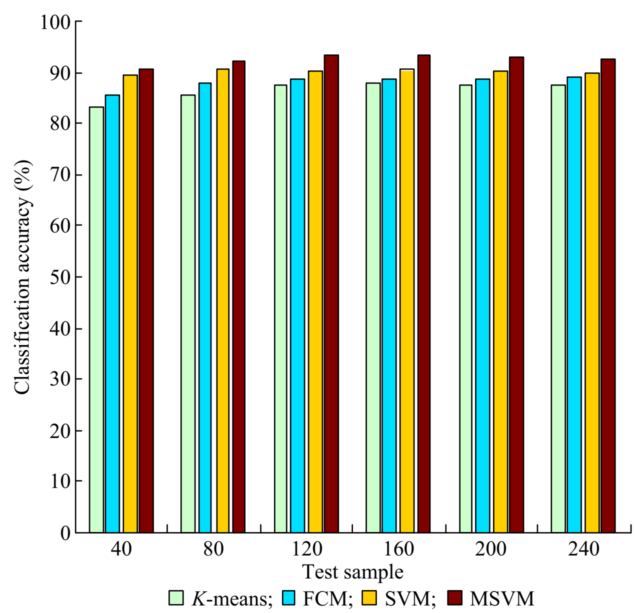

Fig. 6 Classification accuracy comparison with different pattern recognition methods

6 Conclusion

This paper presents a novel fault diagnosis method for a wind turbine bearing based on SSI and MSVM. The SSI method directly constructs a model based on time-domain data and can identify the mode parameters. This is suitable for extracting the fault features. The MSVM is an improved mode recognition method which combines the Gauss kernel SVM and the polynomial kernel SVM, so it can identify the fault types of bearing more accurately.

The results indicate that the SSI-MSVM method is an effective fault diagnosis method for a wind turbine bearing, and can successfully identify fault types of bearing and achieve higher diagnostic accuracy than that of *K*-means clustering, FCM and traditional SVM.

Acknowledgment This work was supported by National Key Technology Research and Development Program (No. 2015BAA06B03).

References

[1] Hang J, Zhang JZ, Cheng M (2014) Fault diagnosis of wind turbine based on multi-sensors information fusion technology. IET Renew Power Gener 8(3):289–298

[2] Wilkinson M, Darnell B, Delft TV et al (2014) Comparison of methods for wind turbine condition monitoring with SCADA data. IET Renew Power Gener 8(4):390–397

[3] Bindi C, Matthews PC, Tavner PJ (2015) Automated on-line fault prognosis for wind turbine pitch system using supervisory control and data acquisition. IET Renew Power Gener 9(5):503–513

[4] Djurovic S, Ceartree CJ, Tavner PJ et al (2012) Condition monitoring of wing turbine induction generators with rotor electrical asymmetry. IET Renew Power Gener 6(4):207–216

[5] Hu AJ, Yan XA, Xiang L (2015) A new wind turbine fault diagnosis method based on ensemble intrinsic time-scale decomposition and WPT-fractal dimension. Renew Energy 83:767–778

[6] Gong X, Qiao W (2013) Bearing fault diagnosis for direct-drive wind turbine via current-demodulated signals. IEEE Trans Ind Electron 60(8):3419–3428

[7] Chen JL, Pan J, Li ZP et al (2016) Generator bearing fault diagnosis for wind turbine via empirical wavelet transform using measured vibration signals. Renew Energy 89:80–92

[8] Sang TH (2010) The self-quality of discrete short-time Fourier transform and its applications. IEEE Trans Signal Process 58(2):604–612

[9] Riera-Guaso M, Antonino-Daviu JA, Pineda-Sanchez M et al (2008) A general approach for the transient detection of slip-dependent fault components based on the discrete wavelet transform. IEEE Trans Ind Electron 55(12):4167–4680

[10] Boashash B (1998) Note on the use of the Wigner distribution for time-frequency analysis. IEEE Trans Acoust Speech Signal Process 36(9):1518–1521

[11] Rai VK, Mohanty AR (2007) Bearing fault diagnosis using FFT of intrinsic mode functions in Hilbert–Huang transform. Mech Syst Signal Process 21:2607–2615

[12] An XL, Jiang DX, Li SH et al (2011) Application of the ensemble empirical mode decomposition and Hilbert transform to pedestal looseness study of direct-drive wind turbine. Energy 30:5508–5520

[13] Liu CL, Wu YJ, Zhen CG (2015) Rolling bearing fault diagnosis based on variational mode decomposition and fuzzy C means clustering. Proc CSEE 35(13):3358–3365

[14] Zhao MY, Xu G (2017) Feature extraction for vibration signals of power transformer based on empirical wavelet transform. Autom Electr Power Syst 41(20):63–69

[15] Bassevill M, Benveniste A, Gach B et al (1993) In situ damage monitoring in vibration mechanics: diagnostics and predictive maintenance. Mech Syst Signal Process 7(5):401–423

[16] Bassevill M, Abdelghani M, Benveniste A (2000) Subspace based fault detection algorithms for vibration monitoring. Automatica 36(1):101–109

[17] Zhou N, Pierre JW, Hauer JF (2006) Initial results in power system identification from injected probing signals using a subspace method. IEEE Trans Power Syst 21(3):1296–1302

[18] Peeters B, Roeck GD (1999) Reference-based stochastic subspace identification for output only modal analysis. Mech Syst Signal Process 13(6):855–878

[19] Nezam SA, Vaithianathan V (2014) Electromechanical mode estimation using recursive adaptive stochastic subspace identification. IEEE Trans Power Syst 29(1):349–358

[20] Gryllias KC, Antoniadis IA (2012) A support vector machine approach based on physical model training for rolling element bearing fault detection in industrial environments. Eng Appl Artif Intell 25(2):326–344

[21] Kang SQ, Li ZQ, Yang GX et al (2014) Application of wavelet packet-locally linear embedding algorithm in rolling bearing fault degree recognization. Chin J Sci Instrum 35(3):614–619

[22] Yao YF, Zhang X (2013) Fault diagnosis approach for roller bearing based on EMD momentary energy entropy and SVM. J Electron Meas Instrum 27(10):957–962

[23] Chen FF, Tang BP, Song T et al (2014) Multi-fault diagnosis study on roller bearing based on multi-kernel support vector machine with chaotic particle swarm optimization. Measurement 47:576–590

[24] Shen ZJ, Chen XF, Zhang XL et al (2012) A novel intelligent gear fault diagnosis model based on EMD and multi-class TSVM. Measurement 45:30–40

[25] Huang J, Hu XG, Geng X (2011) An intelligent fault diagnosis method of high voltage circuit breaker based on improved EMD energy entropy and multi-class support vector machine. Electr Power Syst Res 81(2):400–407

Hongshan ZHAO received the Ph.D. degree from North China Electric Power University, China, in 2004, in electrical engineering. He is now a full professor with the North China Electric Power University, Baoding, China. His research interests include dynamic analysis and control of power system, fault prediction, and optimized maintenance of power system.

Yufeng GAO is currently pursuing the M.S. degree in electrical engineering at North China Electric Power University. His current research interests include fault detection and fault diagnosis of transformer.

Huihai LIU is currently pursuing the M.S. degree in electrical engineering at North China Electric Power University. His current research interests include fault detection and fault diagnosis of wind turbine.

Lang LI received the M.S. degree from North China Electric Power University, China, in 2017. His main research interests include fault detection and maintenance strategy of wind turbine.